Am J Physiol Gastrointest Liver Physiol 292: G939–G951, 2007.
First published October 26, 2006; doi:10.1152/ajpgi.00308.2006.

Effect of SCP-x gene ablation on branched-chain fatty acid metabolism

Barbara P. Atshaves,[1] Avery L. McIntosh,[1] Danilo Landrock,[2] H. Ross Payne,[2] John T. Mackie,[2] Nobuyo Maeda,[3] Judith Ball,[2] Friedhelm Schroeder,[1] and Ann B. Kier[3]

Departments of [1]Physiology and Pharmacology and [2]Pathobiology, Texas A&M University, College Station, Texas; and [3]Department of Pathology, University of North Carolina, Chapel Hill, North Carolina

Submitted 12 July 2006; accepted in final form 21 October 2006

Atshaves BP, McIntosh AL, Landrock D, Payne HR, Mackie JT, Maeda N, Ball J, Schroeder F, Kier AB. Effect of SCP-x gene ablation on branched-chain fatty acid metabolism. *Am J Physiol Gastrointest Liver Physiol* 292: G939–G951, 2007. First published October 26, 2006; doi:10.1152/ajpgi.00308.2006.—Despite the importance of peroxisomal oxidation in branched-chain lipid (phytol, cholesterol) detoxification, little is known regarding the factors regulating the peroxisomal uptake, targeting, and metabolism of these lipids. Although in vitro data suggest that sterol carrier protein (SCP)-x plays an important role in branched-chain lipid oxidation, the full physiological significance of this peroxisomal enzyme is not completely clear. To begin to resolve this issue, SCP-x-null mice were generated by gene ablation of SCP-x from the SCP-x/SCP-2 gene and fed a phytol-enriched diet to characterize the effects of lipid overload in a system with minimal 2/3-oxoacyl-CoA thiolytic activity. It was shown that SCP-x gene ablation *1*) did not result in reduced expression of SCP-2 (previously thought to be derived in considerable part by posttranslational cleavage of SCP-x); *2*) increased expression levels of key enzymes involved in α- and β-oxidation; and *3*) altered lipid distributions, leading to decreased hepatic fatty acid and triglyceride levels. In response to dietary phytol, lack of SCP-x resulted in *1*) accumulation of phytol metabolites despite substantial upregulation of hepatic peroxisomal and mitochondrial enzymes; *2*) reduced body weight gain and fat tissue mass; and *3*) hepatic enlargement, increased mottling, and necrosis. In summary, the present work with SCP-x gene-ablated mice demonstrates, for the first time, a direct physiological relationship between lack of SCP-x and decreased ability to metabolize branched-chain lipids.

sterol carrier protein x; gene targeting; sterol carrier protein 2; liver fatty acid binding protein; phytanic acid

MAMMALS absorb substantial amounts of branched-chain lipids from their diets, including phytanic acid (50–100 mg/day) (for a review, see Ref. 43) and cholesterol (several hundred mg/day) (for a review, see Ref. 42). A variety of peroxisomal disorders involve the inability to oxidize branched-chain fatty acids (BCFAs), leading to elevated levels of phytanic acid and toxicity (for reviews, see Refs. 33 and 45). To prevent the accumulation of toxic branched-chain metabolites, removal by oxidation is essential. Recent data suggest that this process is in part facilitated by sterol carrier protein (SCP)-x and SCP-2, proteins encoded from independent promoters of the SCP-x/SCP-2 gene (19). However, while the SCP-x/SCP-2 gene is organized such that SCP-x contains SCP-2 entirely in the COOH-terminus (for a review, see Ref. 19), it is still not completely clear whether SCP-2 is formed exclusively by a distinct initiation site or by posttranslational cleavage from SCP-x (for a review, see Ref. 19).

Phytanic acid, derived mainly from the diet, is transported to peroxisomes by lipid binding proteins such as extraperoxisomal SCP-2 or liver fatty acid binding protein (L-FABP) (19). Translocation across the peroxisomal membrane occurs after the activation to phytanoyl-CoA, facilitated by an as yet incompletely understood mechanism most likely involving SCP-2 (38). Within peroxisomes, phytanoyl-CoA undergoes several cycles of α- and β-oxidation, followed by transfer of the shortened chain products to mitochondria for the completion of oxidation (45). Several experiments have suggested that the latter steps are facilitated by both SCP-x and SCP-2. In vitro purified SCP-x is a thiolase enzyme that, unlike other known peroxisomal thiolases, has high activity in catalyzing the thiolytic cleavage of 3-oxoacyl-CoA esters of branched-chain molecules with methyl branches at the 2-position (e.g., phytanic acid derivatives) (2, 39). In contrast, while SCP-2 does not exhibit enzymatic activity, it does exhibit high affinity for BCFAs and their CoA derivatives (for a review, see Ref. 18). Moreover, within peroxisomes, SCP-2 interacts with multiple peroxisomal enzymes involved in BCFA oxidation (49). Studies (7, 8) with transfected cells overexpressing SCP-x or SCP-2 have confirmed that both proteins participate in BCFA oxidation. Despite these findings, the physiological relevance of SCP-x and SCP-2 in the oxidation of BCFAs has not been clearly resolved. For example, when both SCP-x and SCP-2 were ablated (41), the resulting SCP-x/SCP-2-null mice showed signs of abnormal phytanic acid oxidation. However, clear interpretation of the results was problematic in that SCP-x/SCP-2 double-knockout mice exhibited loss of both gene products (SCP-x and SCP-2) rather than just SCP-x and L-FABP was concomitantly upregulated four- to fivefold. Since it is now known that phytanic acid oxidation is significantly altered in transfected cells overexpressing L-FABP (7, 8) and in livers and hepatocytes of L-FABP gene-ablated mice (3, 4), it remains unclear whether the abnormal fatty acid oxidation in SCP-x/SCP-2 double-knockout mice was due to the absence of SCP-x, the absence of SCP-2, and/or the upregulation of L-FABP. Efforts to begin to clarify the physiological role of SCP-x in branched-chain lipid metabolism were recently undertaken using female C57BL/6NCr mice with inherently lower hepatic levels of SCP-x protein and no significant fold difference in levels of SCP-2 or L-FABP protein compared with their male counterparts (5). Female mice were found to be more susceptible to dietary phytol stress resulting in weight loss, increased hepatic lesions, altered hepatic lipid distribution, and accumulation of phytol metabolites compared with phytol-fed male and control diet-fed mice. However, it

Address for reprint requests and other correspondence: A. B. Kier, Dept. of Pathobiology, Texas A&M Univ., TVMC, College Station, TX 77843–4467 (e-mail: akier@cvm.tamu.edu).

The costs of publication of this article were defrayed in part by the payment of page charges. The article must therefore be hereby marked "*advertisement*" in accordance with 18 U.S.C. Section 1734 solely to indicate this fact.

remains unclear whether these findings were due to reduced levels of SCP-x or other gender-related factors. The present work was undertaken to delineate the role of SCP-x in BCFA metabolism independent of SCP-2 ablation or substantial upregulation of L-FABP. To begin to resolve these issues, a mouse model null in SCP-x but not SCP-2 was employed to investigate peroxisomal phytanic acid metabolism and lipid distribution in response to dietary phytol.

MATERIALS AND METHODS

Materials. Lipid standards were purchased from Nu-Chek Prep (Elysian, MN) and Avanti (Alabasta, AL). Phytanic acid and phytol were purchased from Sigma (St. Louis, MO). Pristanic acid was a gift from Dr. Herman J. ten Brink (Free University Hospital, Amsterdam, The Netherlands). Rabbit polyclonal anti-catalase was purchased from Biodesign (Kennebunk, ME). Monoclonal anti-GAPDH was from Millipore (Billerica, MA). Rabbit polyclonal anti-fatty acid transport protein (FATP)-1 was a generous gift from Dr. J. Schaffer (Department of Internal Medicine, Washington University School of Medicine, St. Louis, MO). Rabbit polyclonal antisera to recombinant rat acyl CoA binding protein (ACBP), porcine glutamic-oxaloacetic transaminase (GOT; also known as aspartate aminotransferase), and rat L-FABP were prepared as previously described (6). A rabbit polyclonal antibody directed against SCP-x recognizing all SCP-x/SCP-2 gene products (58-kDa SCP-x, 46-kDa thiolase, 15-kDa pro-SCP-2, and 13.2-kDa SCP-2) was prepared as previously described (5).

Animals. All animal protocols were approved by the Institutional Animal Care and Use Committee at Texas A&M University. Male and female (6 wk old, 20–30 g) inbred C57BL/6NCr mice were obtained from the National Cancer Institute (Frederick Cancer Research and Developmental Center, Frederick, MD). SCP-x gene-ablated mice were generated as described below (*Generation of SCP-x gene-ablated mice*). Unless used for the phytol dietary study, all mice were maintained on standard rodent chow mix (5% calories from fat). Mice were kept under a 12:12-h light-dark cycle in a temperature-controlled facility (25°C) with access to food and water ad libitum. For antibody production, adult female New Zealand White (specific pathogen free) rabbits (2 kg) were obtained from Harlan (Indianapolis, IN). Rabbits were maintained on standard rabbit chow mix (Teklad, Harlan), given free access to food and water, and kept on a constant light cycle of 12:12-h light-dark. Animals in the facility were monitored quarterly for infectious diseases.

Generation of SCP-x gene-ablated mice. SCP-x-null mice were generated by targeted disruption of the SCP-x gene through homologous recombination. Primers (5′-CCCGACGCCTGGGGTTGGA-TAA-3′ and 5′-CTTGGTCATGCCAACGCCGACC-3′) were designed to amplify a 150-bp fragment from mouse DNA that included exon 1 of the SCP-x gene. The 150-bp amplicon was used to screen a genomic 129/sv Lambda FIX library (Stratagene, La Jolla, CA). Positive clones were confirmed by extensive restriction mapping and sequence analysis. Two overlapping genomic DNA fragments, a 4.5-kb *Sac*I clone (containing exon 1 and surrounding intronic sequences) and a 4.5-kb *Bam*HI/*Eco*RI clone (containing intronic sequences immediately upstream of exon 1), formed the backbone of the targeting construct. The 3′ homology arm was generated by ligating a blunt-ended 1.8-kb *Bgl*II fragment from the 4.5-kb *Sac*I clone into pBluescript II SK (+) vector (Stratagene) predigested with *Sma*I. The length of the 3′ arm was increased by digesting the resultant plasmid with *Pst*I and ligation with a 1.1-kb *Pst*I fragment from the 4.5-kb *Bam*HI/*Eco*RI clone to yield a 2.1-kb 3′ homology region with a *Bam*HI site at the 5′ end. The 3′ fragment was introduced into the targeting vector pKO Scrambler NTKV-1901 (Stratagene), a plasmid carrying the neomycin resistance marker, using *Bam*HI/*Eco*RI sites to yield an intermediate targeting construct. The targeting construct was completed by ligating the 5′ arm (a 2.6-kb fragment derived by digesting the 4.5-kb *Bam*HI/*Eco*RI clone with *Hin*dIII/*Eco*RI) into the intermediate targeting construct predigested with *Hin*dIII/*Eco*RI. Once complete, the targeting construct was opened with *Not*I and electroporated into 129/Ola-derived embryonic stem cell line E14 (23) maintained on feeder layers. After selection with G418 (200 μg/ml) and gancyclovir (2 μM), DNA was isolated from surviving clones, digested with *Bam*HI, and screened by Southern blot analysis following standard protocols (30). Using a 230-bp 5′ probe external to the targeting construct, targeted clones were identified by the presence of a 6-kb band resulting from replacing exon 1 with the neomycin cassette of pKO Scrambler NTKV-1901. Two positive clones were expanded and injected into C57BL/6NCr blastocysts to create chimeric mice following standard procedures (13). Three male chimeras were identified by coat color and bred to C57BL/6NCr females to determine germ line transmission of the targeted allele. Tail DNA from F1 offspring with mixed coat color (agouti) was screened by PCR to verify the genotype of each animal. Initial characterization of the SCP-x gene ablation by Western blot analysis was performed on F2 SCP-$x^{-/-}$ homozygous mice generated by interbreeding heterozygous F1 animals. Subsequently, heterozygous F1 animals were backcrossed to the N4 C57BL/6NCr background before being interbred to produce the SCP-x-null and wild-type mice used in the present study.

Antibody production. Peroxisomal thiolases A and B (pThiol) were distinguished from SCP-x by preparing rabbit polyclonal antisera to specific nonoverlapping peptides that were synthesized by standard fluorenylmethoxycarbonyl solid-phase chemistry (Peptide Synthesis Core Facility, Texas A&M University, directed by Dr. Judith Ball) employing a Millipore 9050 Plus automated peptide synthesizer (Perceptive Biosystems, Framingham, MA) as previously described (24). Two peptide antibodies were prepared. One peptide antibody detected SCP-x but not pThiol or SCP-2. This peptide antibody was prepared against a synthetic peptide (KFMKPGGENSRDYPD-MAKEAG) comprising amino acids 23–43 of SCP-x, similar to that previously prepared by others (35). The second antibody detected pThiol but not SCP-x or SCP-2. This peptide antibody was prepared against a 21-amino acid synthetic peptide DEGVRPSTTMEGLAK-LKPAFK (comprising amino acids 255–275 of thiolase A).

Dietary (phytol) experiments. One week before the start of the feeding experiments, male and female mice (2 mo of age, 20–30 g) were switched to a modified AIN-76A phytol-free, phytoestrogen-free rodent diet (5% calories from fat, diet no. D11243, Research Diets, New Brunswick, NJ). This diet was chosen because standard rodent chow contained significant amounts of both phytol and phytanic acid (41) and phytoestrogens (4), which could complicate the gender-based and phytol effect comparisons within the study. Each mouse was housed individually in Tecniplast Sealsafe IVC cages (365 mm width × 207 mm depth × 140 mm height) with external water bottles and wire bar lid holders containing food pellets. After 1 wk, one-half of the mice remained on the phytol-free diet, whereas the rest were switched to a modified AIN-76A rodent diet supplemented with 0.5% phytol (5% calories from fat, diet no. D01020601, Research Diets). Animal body weights and food intake were monitored every other day as follows: at similar times of the day (midmorning), each mouse was removed from the cage, examined briefly, placed in a beaker, and then weighed. In the cage, food pellets from the food holder and bedding (strained to gather smaller pellets that had fallen through the lid mesh) were also weighed. Since the food was color coded (yellow for control food and pink for 0.5% phytol), pellets were clearly visible and not easily missed. At the end of the study (*day 14*), animals were fasted overnight and anesthetized (100 mg/kg ketamine and 10 mg/kg xylaxine), and blood was collected by cardiac puncture. Whole body dual-energy X-ray absorptiometry (DEXA) using a Lunar PIXImus densitometer (Lunar, Madison, WI) was performed to determine the fat tissue mass (FTM) and lean tissue mass (LTM) as previously described (4, 5). Livers were harvested and weighed, and several livers from each feeding group were immediately photographed as

described in Ref. 5. Liver slices were excised for light microscopy and histological examination with the remaining portions snap frozen on dry ice and stored at −80°C for lipid and Western blot analyses.

Histopathology. Liver slices were excised near the porta hepatis and fixed in 10% neutral-buffered formalin for 24–48 h. Tissues were then transferred to 70% ethyl alcohol, processed, and embedded in paraffin. Liver sections (5 μm thick) were stained with hematoxylin and eosin (H&E) for histological examination under a light microscope. To stain lipid droplets in the liver samples, sections (1- to 2-mm^3 segments) were also fixed by immersion in glutaraldehyde and formaldehyde at room temperature as described in Ref. 20 with slight modifications. Briefly, liver tissue was incubated for 5 h in 1% osmium tetroxide and 2.5% potassium dichromate, dehydrated in a graded ethanol series, and embedded in Spurr's epoxy resin. Semithin sections (0.75 μm thick) were mounted on glass slides, coverslipped, and examined without being counterstained. Liver sections were imaged with a ×40 light microscope objective and recorded with a charge-coupled device (CCD) camera. Representative images were randomly selected from each liver for a total image area of 0.8 mm^2 per treatment group.

Lipid mass determination. Hepatic lipids were extracted with 3:2 (vol/vol) *n*-hexane-2-propanol (21) and immediately stored under an atmosphere of N_2 to limit oxidation. Protein content was determined by the method of Bradford (12) from the dried protein residue digested overnight in 0.2 M KOH. The lipid extract was divided into portions for lipid mass and fatty acid composition determination as previously described (3). Phospholipids and neutral lipids [cholesterol, free fatty acids (FFAs), triacylglycerol (TG), and cholesterol ester (CE)] were resolved using silica gel G thin-layer chromatography (TLC) plates developed in the following solvent system: petroleum ether-diethyl ether-methanol-acetic acid (90:7:2:0.5) (3). Lipids were identified by comparison to known standards. TLC spots were visualized by iodine, scraped, and quantitated by the method of Marzo et al. (31). All glassware was washed with sulfuric acid-chromate before being used.

Fatty acid composition. Acid-catalyzed transesterification was performed on the remaining portion of the extracted lipid fraction described above to convert the lipid acyl chains to fatty acid methyl esters (FAMEs) (4, 5). FAMEs were extracted into *n*-hexane and separated by gas-liquid chromotography on a GLC-14A (Shimadzu, Kyoto, Japan) equipped with a RTX-2330 capillary column (0.32 mm inner diameter × 30 m length, Restek, Bellefonte, PA) with the injector and detector temperatures set at 260°C. A Waters SAT/IN analytical-to-digital interface was used to collect peak area data, which were converted to peak area data using Millenium^{32} 3.2 software. Individual peaks were identified by comparison to known FAME standards (Nu-Chek) referenced to a set concentration of 15:0 added before analysis. Phytol metabolites (phytanic acid, pristanic acid, and $\Delta^{2,3}$-pristenoic acid) were confirmed by gas chromatography/mass spectroscopy (GC/MS) on a Trace DSQ single quadrapole GC/MS with electron impact and chemical ionization sources (Thermo Electron, Austin, TX) in chemical ionization mode.

Western blot analysis. Expression of intracellular FATPs (L-FABP, SCP-2, and ACBP), plasma membrane FATPs (FATP-1 and GOT), and peroxisomal enzymes (SCP-x, pThiol, and catalase) were determined by Western blot analysis as described in (6). Briefly, since each protein of interest and the housekeeping gene GAPDH was easily resolved by size on the tricine gels, membranes were cut into two so that each Western blot was probed with antisera against the protein of choice and GAPDH to ensure uniform protein loading. Alkaline-phosphatase conjugates of goat anti-rabbit or mouse IgG and Sigma Fast 5-bromo-4-chloro-3-indolyl phosphate/nitroblue tetrazolium tablets (Sigma) were used to visualize protein bands. Proteins were quantified by densitometric analysis after image acquisition using a single-chip CCD video camera and a computer workstation (IS-500 system, Alpha Innotech, San Leandro, CA). Image files were analyzed (mean 8-bit grayscale density) using NIH Image (available by anonymous FTP). Expression of each protein was normalized to the mean expression of GAPDH. For quantitative analysis, linear standard curves were generated from Western blots where pure protein was available (SCP-x, SCP-2, L-FABP, and ACBP). Band intensities on the Western blots were analyzed as described above and then plotted against the protein amount to generate a standard curve within the linear range of each protein. Changes in protein expression between liver homogenate samples were quantitated by comparing the sample with the standard curve on each blot. Proteins with no source of pure protein available (FATP-1, GOT, and catalase) were expressed as fold differences between samples.

Real-time PCR. Real-time PCR was performed on total RNA from livers isolated and purified using a RNeasy minikit (Qiagen,Valencia, CA) in accordance with the manufacturer's protocol. RNA concentrations were determined spectrophotometrically, and their integrity was verified by agarose electrophoresis and ethidium bromide staining. For quantitative real-time PCR, expression patterns were analyzed with an ABI PRISM 7000 Sequence Detection System (Applied Biosystems, Foster City, CA) using the TaqMan One Step PCR Master Mix Reagent kit, gene-specific TaqMan PCR probes and primers, and the following thermal cycler protocol: 48°C for 30 min, 95°C for 10 min before the first cycle, 95°C for 15 s, and 60°C for 1 min, repeated 40 times. Using TaqMan One Step chemistry, total RNA was reverse transcribed in the first step of the thermal cycler protocol (48°C for 30 min) before amplification. For specific probes and primers, Assay-on-Demand products for mouse pristanoyl CoA oxidase ($ACO_{pristanoyl}$; Mm00446122_m1), liver peroxisomal bifunctional enzyme (PBE; Mm00470091_m1), phytanoyl hydroxylase (Phyh; Mm00477734_m1), mitochondrial 3-oxoacyl CoA thiolase (mThiol; Mm00624282_m1), short-chain acyl (butyryl) CoA dehydrogenase (mButCoADH; Mm00431617_m1), and carnitine palmitoyl CoA acyltransferase 1 (CpT1; Mm00550438_m1) were obtained from Applied Biosystems. Experiments were performed in triplicate and analyzed with ABI Prism 7000 SDS software (Applied Biosystems) to determine the threshold cycle (C_T) from each well. Primer concentrations and cycle number were optimized to ensure that the reactions were analyzed in the linear phase of amplification. To analyze real-time PCR data, mRNA expression of $ACO_{pristanoyl}$, PBE, Phyh, mThiol, mButCoADH, and CpT1 in the different mice groups (including female wild-type mice on the control diet, male and female SCP-x-null mice on the control diet, male and female wild-type mice on the phytol diet, and male and female SCP-x-null mice on the phytol diet) were normalized to a housekeeping gene (18S RNA) and made relative to the control mouse group (male wild-type mice on the control diet). Values were calculated using the comparative $2^{-\Delta\Delta C_T}$ method (26) where $\Delta\Delta C_T$ = [C_T of the target gene − C_T of 18S RNA] of the different mice groups − [C_T of the target gene − C_T of 18S RNA] of the control mouse group, as described in User Bulletin 2, ABI Prism 7000 Sequence Detection System (Applied Biosystems), and Ref. 26.

Statistics. Each feeding group consisted of five to seven animals. All values are expressed as means ± SE. Statistical analysis was performed using ANOVA combined with the Newman-Keuls multiple-comparisons test (GraphPad Prism, San Diego, CA). Values with $P < 0.05$ were considered statistically significant.

RESULTS

Generation of SCP-x gene-ablated mice. To generate 58-kDa SCP-x-null mice that retained the ability to express 15.2-kDa pro-SCP-2 and 13.2-kDa SCP-2 proteins, a targeting construct was designed that replaced exon 1 of the SCP-x/SCP-2 gene with a neomyocin cassette (Fig. 1). This design allowed the expression of SCP-2 from the second promoter of the SCP-x/SCP-2 gene. Gene-targeted mice were screened by PCR for genotyping (Fig. 1*C*) and Western blot analysis (Fig.

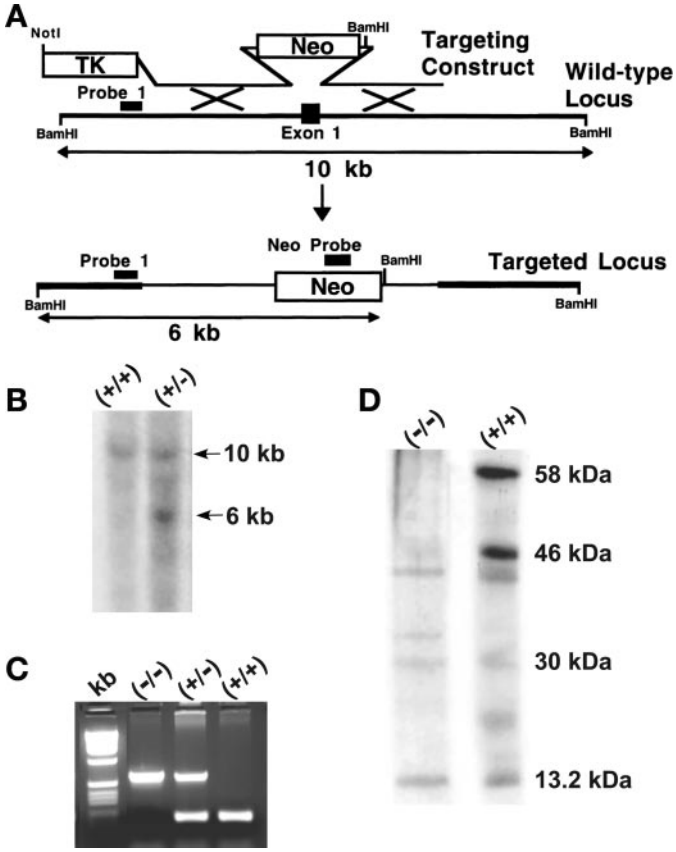

Fig. 1. Generation of the sterol carrier protein (SCP)-x-null mouse. *A*: targeted mutation of the SCP-x gene is indicated in the *top* diagram, where exon 1 is replaced by the neomycin resistance cassette (Neo) through homologous recombination. The *bottom* diagram shows the mutated SCP-x gene with *Bam*HI sites and the external *probe 1* and Neo probe indicated. TK, thymadine kinase gene. *B*: Southern blot of *Bam*HI-digested DNA probed with external *probe 1* shows the wild-type (WT; 10 kb) and targeted (6 kb) DNA. *C*: PCR screening of tail DNA from WT SCP-$x^{+/+}$, heterozygous SCP-$x^{+/-}$, and homozygous SCP-$x^{-/-}$ mice. *D*: Western blots of liver cell homogenates (5 μg) from male SCP-$x^{-/-}$ and WT SCP-$x^{+/+}$ mice were probed with an affinity-purified rabbit polyclonal antibody directed against SCP-x recognizing all SCP-x/SCP-2 gene products (SCP-x, 46-kDa thiolase, and SCP-2).

1*D*) using an antibody reactive to all forms of SCP-2 (58-kDa SCP-x, 46-kDa thiolase, 15-kDa pro-SCP-2, and 13.2-kDa SCP-2) to verify the lack of SCP-x expression. As predicted from the construct design, 58-kDa SCP-x and 46-kDa thiolase enzymes were absent in livers from SCP-$x^{-/-}$ mice, whereas 13.2-kDa SCP-2 protein was still present (Fig. 1*D*). Thus, SCP-x gene ablation was confirmed in SCP-$x^{-/-}$ homozygous mice.

Contribution of SCP-x to SCP-2 expression. If a significant proportion of 13.2-kDa SCP-2 was attributed to the posttranslational cleavage of 58-kDa SCP-x, then it was expected that levels of 13.2-kDa SCP-2 would be substantially decreased in SCP-$x^{-/-}$ mice. On the contrary, quantitative analysis of multiple Western blots (normalized to the housekeeping gene GAPDH) indicated that levels of 13.2-kDa SCP-2 were not decreased in liver homogenates of male SCP-$x^{-/-}$ mice; rather, they were increased 2.5-fold (Fig. 2*B*). Furthermore, levels of 13.2-kDa SCP-2 in female SCP-$x^{-/-}$ mice were increased more so, 5.4-fold (from 1.6 ± 0.1 to 8.6 ± 0.9 ng/μg protein, $n = 5$–7), where quantitative analysis was performed using standard curves of recombinant protein (13.2-kDa SCP-2) loaded on blots along with liver homogenate samples as described in MATERIALS AND METHODS (data not shown). Taken together, these data show that *1*) SCP-x gene ablation did not elicit SCP-2 ablation, *2*) SCP-x was not the major source of 13.2-kDa SCP-2, and *3*) 13.2-kDa SCP-2 expression was upregulated in a gender-dependent manner.

Effect of SCP-x gene ablation on whole body phenotype and lipids. Male and female SCP-x-null mice did not show any evidence of abnormal appearance, viability, or behavior. Liver and body weights of 10-wk-old male and female SCP-$x^{-/-}$ mice were not significantly different from their wild-type (SCP-$x^{+/+}$) littermates (Table 1), and the gross morphology of livers from male and female SCP-$x^{-/-}$ mice was also essentially normal. Consistent with these results, there were no significant differences in body weights or percent changes in body weight in SCP-$x^{-/-}$ versus wild-type SCP-$x^{+/+}$ mice fed the control diet (Fig. 3, *E* and *F*). To determine if SCP-x gene ablation altered the proportion of FTM and/or LTM, DEXA was performed. DEXA scans revealed that SCP-x gene ablation alone did not significantly alter the proportion of FTM (Fig. 4*C*, crosshatched bar) or LTM (Fig. 4*D*, crosshatched bar) in male or female mice compared with wild-type counterparts. Thus, SCP-x gene ablation alone did not alter the whole body phenotype (food consumption, body weight, FTM, or LTM).

To define the effects of SCP-x gene ablation on liver and serum lipid parameters, lipids were extracted, and levels of TG, FFAs, cholesterol, and CE were determined in fasting mice. Fasting serum levels of TG in male SCP-$x^{-/-}$ mice were significantly decreased compared with their wild-type (SCP-$x^{+/+}$) littermates, with a similar trend observed in female SCP-$x^{-/-}$ mice (Table 1). With FFA levels, serum levels were not significantly different in male or female SCP-x-null mice. Serum levels of cholesterol were significantly increased in male SCP-$x^{-/-}$ mice, whereas levels of cholesterol plus CE (total cholesterol) were similar to male SCP-$x^{+/+}$ animals. In female SCP-$x^{-/-}$ mice, serum levels of cholesterol and total cholesterol were not significantly different from their wild-type counterparts (Table 1).

Liver lipid parameters were also affected by SCP-x gene ablation. Liver TG was decreased, especially in female SCP-$x^{-/-}$ mice (1.7-fold, $P < 0.04$), reflecting the decreased levels of FFAs in both male and female SCP-$x^{-/-}$ mice (Table 1). Hepatic cholesterol and total cholesterol levels in male, but not female, SCP-$x^{-/-}$ mice were decreased slightly (23% and 20%, respectively, $P < 0.05$), whereas CE levels were not significantly changed in either male or female SCP-x mice (Table 1). Overall, despite the minimal changes in the whole body phenotype (body weight, FTM, and LTM), the serum and liver lipid phenotype in SCP-$x^{-/-}$ mice was significantly altered in a gender-dependent manner, whereas an altered FFA, rather than cholesterol, metabolic phenotype was observed in SCP-x gene-ablated mice.

Effect of SCP-x gene ablation on intracellular transport proteins. Since upregulation of the intracellular FATP SCP-2 was observed in SCP-x-null mice, the effect of SCP-x gene ablation on levels of other FATPs was determined. As described in MATERIALS AND METHODS, quantitative analysis of multiple Western blots normalized to the housekeeping gene GAPDH (Fig. 2*H*) showed that SCP-x gene ablation did not upregulate L-FABP expression in male mice but instead de-

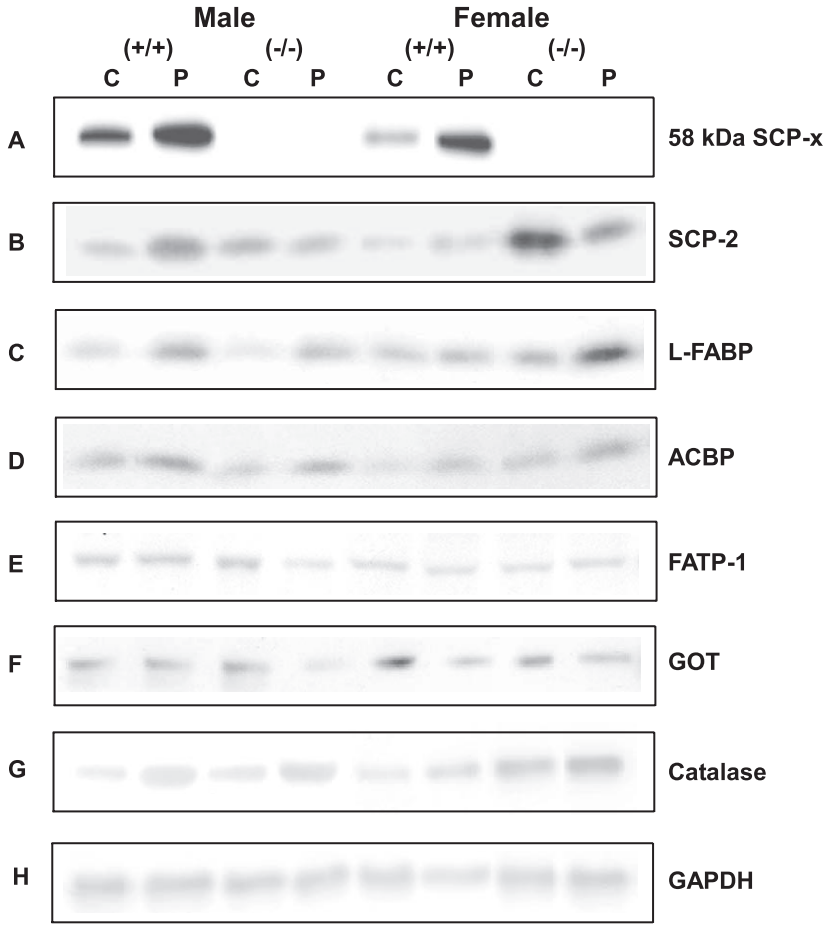

Fig. 2. Representative Western blots of liver proteins in male and female WT SCP-$x^{+/+}$ and SCP-$x^{-/-}$ knockout (KO) mice fed a defined diet with or without 0.5% phytol [control diet (C) and phytol diet (P)]. Western blots of liver cell homogenates (2 μg) were probed with the following affinity-purified antibodies as described in MATERIALS AND METHODS: anti-58-kDa SCP-x (*A*), anti-SCP-2 (*B*), anti-liver fatty acid binding protein (L-FABP; *C*), anti-acyl CoA binding protein (ACBP; *D*), anti-fatty acid transport protein 1 (FATP-1; *E*), anti-glutamic-oxaloacetic transaminase (GOT; *F*), anti-catalase (*G*), and anti-GAPDH (*H*). The GAPDH signal was used as a loading control to normalize protein expression.

creased L-FABP expression by 69% (Fig. 2*C*), from 2.7 ± 0.2 to 0.83 ± 0.1 ng/μg liver homogenate protein ($P < 0.001$, $n = 4$). In contrast, levels of L-FABP in female SCP-$x^{-/-}$ mice were increased twofold, from 1.4 ± 0.3 to 2.8 ± 0.4 ng/μg liver homogenate ($P < 0.001$, $n = 4$). SCP-x gene ablation also decreased levels of ACBP (Fig. 2*D*) in liver homogenates of male mice (39%, from 1.20 ± 0.06 to 0.73 ± 0.02 ng/μg, $P < 0.001$, $n = 4$) but increased levels in female mice by 1.6-fold, from 1.6 ± 0.2 to 2.6 ± 0.1 ng/μg liver homogenate ($P < 0.001$, $n = 4$). In contrast, expression of plasma membrane FATPs, including FATP-1 and GOT (9–11, 15), were unaltered in male SCP-$x^{-/-}$ mice (Fig. 2, *E* and *F*) and altered only slightly (i.e., FATP-1 unaltered and GOT decreased by 38%) in female SCP-$x^{-/-}$ mice. Taken together, these data suggest that any alterations in liver fatty acid metabolism associated with SCP-x gene ablation were not due to altered levels of plasma membrane FATPs but may in part be determined by gender-dependent alterations in levels of intracellular cytosolic fatty acid/fatty acyl CoA transport proteins (L-FABP and ACBP).

Table 1. *Effect of SCP-x gene ablation on whole body phenotype and serum and liver lipid parameters*

Parameters	Male		Female	
	SCP-$x^{+/+}$	SCP-$x^{-/-}$	SCP-$x^{+/+}$	SCP-$x^{-/-}$
Liver, g	0.90±0.05	1.0±0.06	0.80±0.02	0.80±0.01
Body weight, g	25.9±0.8	26.3±0.9	20.7±0.5	19.2±0.2
Serum, nmol/mg protein				
Cholesterol	11±1	18±2*	11±1	14±1
Cholesterol ester	46±4	47±5	30±3	31±2
Triacylglycerol	8±2	3±1*	4.0±0.9	3.2±0.5
Free fatty acids	21±1	29±14	28±5	22±2
Liver, nmol/mg protein				
Phospholipid	120±8	148±22	269±17	251±20
Cholesterol	66±5	51±3*	53±4	43±5
Cholesterol ester	27±2	23±3	66±10	72±12
Triacylglycerol	147±17	107±12	265±24	154±25†
Free fatty acids	129±14	79±4	216±17	163±14†

Values are means ± SE; n = 5–10 (12 wk old) mice/group. SCP-x, sterol carrier protein x. *P<0.04 vs. male wild-type SCP-$x^{+/+}$ mice; †P<0.04 vs. female wild-type SCP-$x^{+/+}$ mice.

Effect of SCP-x gene ablation on key peroxisomal enzymes. To determine if SCP-x gene ablation altered the expression levels of key peroxisomal fatty acid oxidative enzymes, real-time PCR and Western blot analysis were performed as described in MATERIALS AND METHODS. The conversion of phytanic acid to pristanic acid is accomplished via an α-oxidation step catalyzed by Phyh (47). Real-time PCR showed that mRNA expression of Phyh was significantly lower (3.7-fold, $P < 0.009$) in female wild-type SCP-$x^{+/+}$ mice compared with males (Fig. 5*A*). In contrast, SCP-x gene ablation increased Phyh gene expression in female SCP-$x^{-/-}$ mice by fourfold ($P < 0.05$) compared with their female wild-type counterparts, with a trend toward the increase observed in male mice. After phytanic acid is α-oxidized to pristanic acid, the first β-oxidation step occurs, catalyzed by $ACO_{pristanoyl}$, an enzyme with

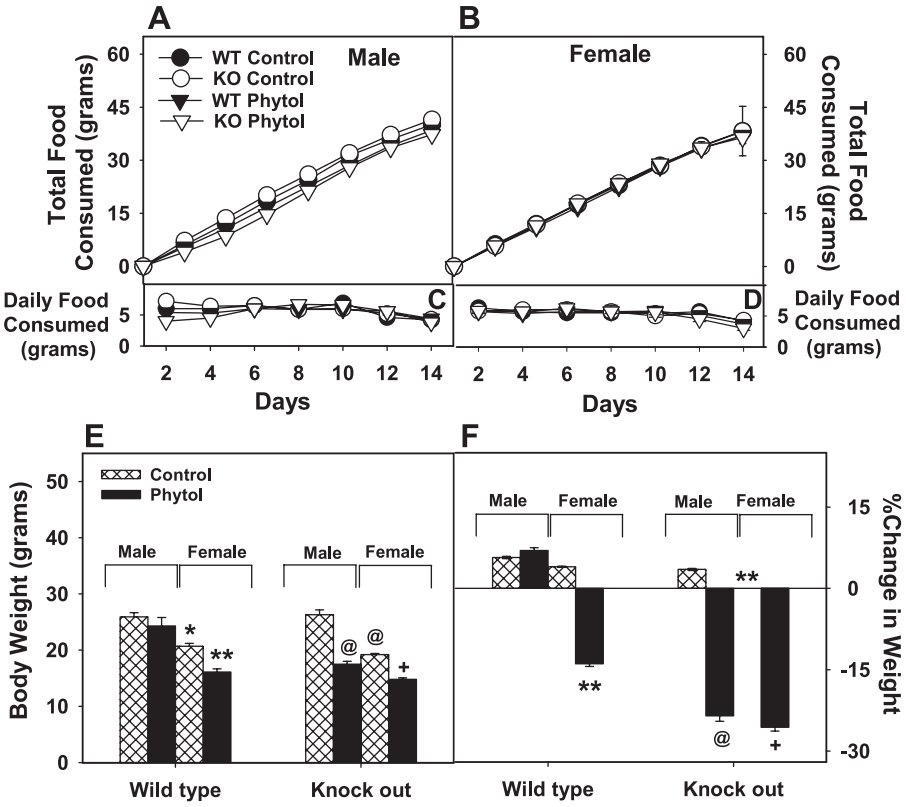

Fig. 3. Food consumption and body weight changes in male and female SCP-$x^{+/+}$ and SCP-$x^{-/-}$ mice fed a defined diet with or without 0.5% phytol. The total food consumption in male (*A*) and female (*B*) mice and daily food consumed in male (*C*) and female (*D*) mice were determined for animals fed control and 0.5% phytol diets as described in MATERIALS AND METHODS. Body weights (*E*) and percent changes in body weights (*D*) for each mouse group at the end of the dietary experiments were also determined. Values represent means ± SE; n = 5–7 animals/group. $^{**}P < 0.05$ vs. female WT SCP-$x^{+/+}$ mice on the control diet; $^{@}P < 0.001$ vs. male SCP-$x^{-/-}$ mice on the control diet; $^{+}P < 0.001$ vs. female SCP-$x^{-/-}$ mice on the control diet.

substrate preference for 2-methyl BCFAs (44). In contrast to Phyh, mRNA expression levels of $ACO_{pristanoyl}$ were not significantly different between male and female SCP-$x^{+/+}$ mice fed the control diet (Fig. 5*B*). In female SCP-$x^{-/-}$ mice, however, expression levels of $ACO_{pristanoyl}$ were decreased by 3.7-fold ($P < 0.05$) compared with wild-type mice. No differences were observed between control diet-fed male SCP-$x^{-/-}$ and wild-type mice. The next two steps of conversion are catalyzed by PBE, a protein composed of several domains with hydratase, dehydrogenase, and lipid binding activity (44). Much like Phyh, not only were expression levels of PBE in female wild-type SCP-$x^{+/+}$ mice decreased significantly (5-fold, $P < 0.009$) compared with control diet-fed wild-type male mice (Fig. 5C) but SCP-x gene ablation increased gene expression in female SCP-$x^{-/-}$ mice by 4.4-fold ($P < 0.05$) compared with their female wild-type counterparts (Fig. 5*C*). The last step in the peroxisomal β-oxidation cycle of fatty acids involves thiolytic cleavage of branched- or straight-chain

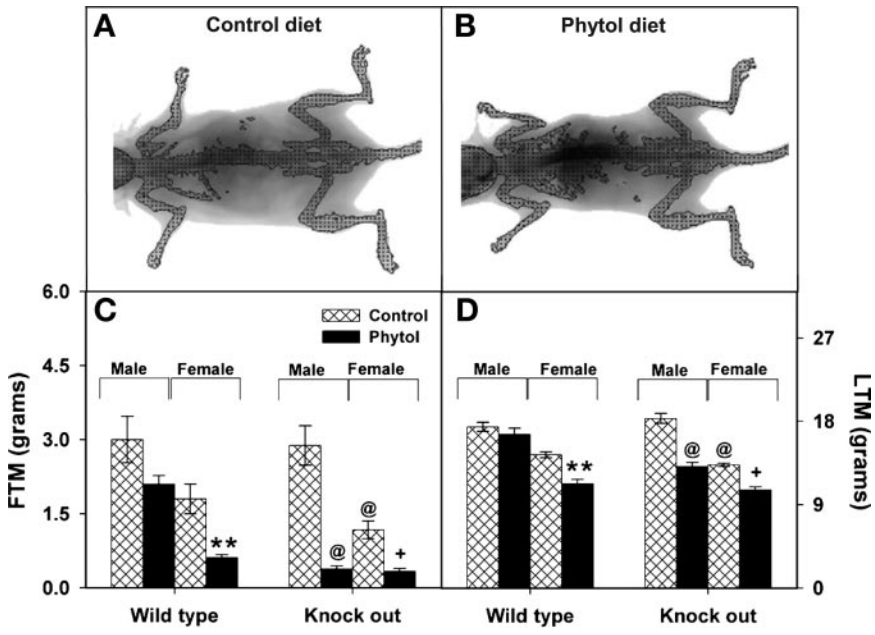

Fig. 4. Distribution of fat tissue mass (FTM) and lean tissue mass (LTM). Representative Lunar PIXImus dual-energy X-ray absorptiometry (DEXA) scans are shown for male SCP-$x^{-/-}$ mice fed control (*A*) and 0.5% phytol (*B*) diets. The percent changes in FTM (*C*) and LTM (*D*) were determined as described in MATERIALS AND METHODS. Values represent means ± SE; n = 5–7 animals/group. $^{**}P < 0.01$ vs. female WT SCP-$x^{+/+}$ mice on the control diet; $^{@}P < 0.004$ vs. male SCP-$x^{-/-}$ mice on the control diet; $^{+}P < 0.001$ vs. female SCP-$x^{-/-}$ mice on the control diet.

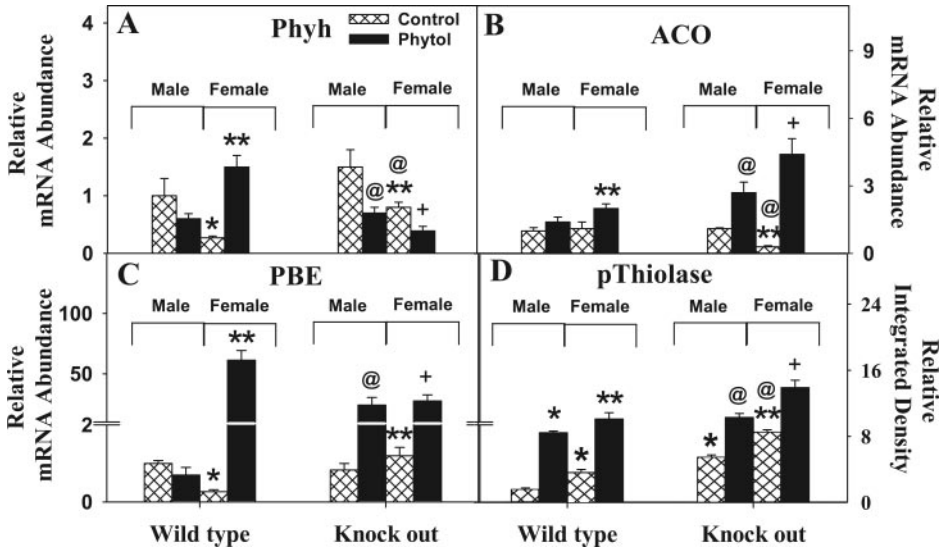

Fig. 5. Relative expression levels of key peroxisomal β-oxidation enzymes. Expression levels of phytanoyl hydroxylase (Phyh; *A*), prisanoyl CoA oxidase (ACO; *B*), peroxisomal bifunctional enzyme (PBE; *C*), and peroxisomal thiolases A and B (pThiolase; *D*) were determined in male and female SCP-x$^{+/+}$ and SCP-x$^{-/-}$ mice on control and 0.5% phytol diets as described in MATERIALS AND METHODS. Values represent means ± SE; n = 5–7 animals/group. *$P <$ 0.009 vs. male WT SCP-x$^{+/+}$ mice on the control diet; **$P < 0.05$ vs. female WT SCP-x$^{+/+}$ mice on the control diet; $^{@}P < 0.05$ vs. male SCP-x$^{-/-}$ mice on the control diet; $^{+}P < 0.007$ vs. female SCP-x$^{-/-}$ mice on the control diet.

molecules via 58-kDa SCP-x or 41-kDa thiolases (pThiol), respectively (44). Using an antibody specific to pThiol, Western blot analysis showed that levels of pThiol in liver homogenates of wild-type SCP-x$^{+/+}$ mice were gender dependent (Fig. 5*D*), where females exhibited 2.3-fold more than males ($P < 0.05$, $n = 4$). In addition, SCP-x gene ablation significantly increased levels of pThiol in liver homogenates of both male and female SCP-x$^{-/-}$ mice by 3.5- and 2.4-fold, respectively (Fig. 5*D*). Thus, SCP-x gene ablation resulted in altered expression of several α- and β-oxidative enzymes, especially in female SCP-x-null mice, with an overall trend toward increased peroxisomal fatty acid oxidation.

Effect of SCP-x gene ablation on key mitochondrial enzymes. Real-time PCR was used to determine the effect of SCP-x gene ablation on key mitochondrial enzymes involved in fatty acid β-oxidation. Livers of female versus male wild-type SCP-x$^{+/+}$ mice expressed two- to threefold lower mRNA levels of the following key enzymes: CpT1, which is involved in the translocation of fatty acid carnitine esters across the mitochondrial membrane; mButCoADH, which is involved in the first step of mitochondrial β-oxidation; and mThiol, which catalyzes the last step of fatty acid β-oxidation in mitochondria (Fig. 6). SCP-x gene ablation decreased CpT1 mRNA expression by 22% ($P < 0.05$) and threefold ($P < 0.001$) in male and female SCP-x$^{-/-}$ mice, respectively (Fig. 6*A*). In contrast, a trend toward decreased mThiol mRNA expression and increased mButCoADH expression (2.5-fold, $P < 0.001$) was observed in male but not female SCP-x$^{-/-}$ mice (Fig. 6, *B* and *C*, respectively). Since CpT1 is the rate-limiting enzyme in mitochondrial fatty acid oxidation, these data suggest that, in general, SCP-x gene ablation altered the expression of multiple mitochondrial proteins toward decreased mitochondrial fatty acid oxidation.

Effect of SCP-x gene ablation and dietary phytol on the whole body phenotype. To determine if a phytol-rich diet altered whole body phenotype, SCP-x$^{-/-}$ and wild-type SCP-x$^{+/+}$ mice were put on a 0.5% phytol diet with food consumption and body weight measured every other day as described in MATERIALS AND METHODS. The dietary experiments were stopped after 14 days because thereafter the phytol-rich diet elicited severe weight loss (Fig. 3, *E* and *F*, filled bars) where female, but not male, wild-type SCP-x$^{+/+}$ mice exhibited a substantial weight loss of 14% ($P < 0.001$, $n = 7$). The response to the phytol diet was even greater in SCP-x gene-ablated mice, where both male and female mice exhibited a 24–26% weight loss ($P < 0.001$) despite similar food consumption (Fig. 3,

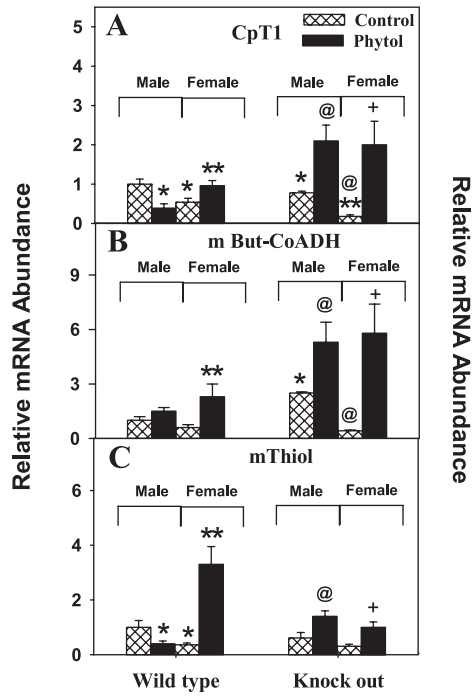

Fig. 6. Relative expression levels of key mitochondrial β-oxidation enzymes. Expression levels of carnitine palmitoyl CaA acyltransferase 1 (CpT1; *A*), short-chain acyl (butyryl) CoA dehydrogenase (mButCoADH; *B*), and mitochondrial 3-oxacyl CoA thiolase (mThiol; *C*) were determined in male and female SCP-x$^{+/+}$ and SCP-x$^{-/-}$ mice on control and 0.5% phytol diets as described in MATERIALS AND METHODS. Values represent means ± SE; n = 5–7 animals/group. *$P < 0.05$ vs. male WT SCP-x$^{+/+}$ mice on the control diet; **$P < 0.003$ vs. female WT SCP-x$^{+/+}$ mice on the control diet; $^{@}P < 0.03$ vs. male SCP-x$^{-/-}$ mice on the control diet; $^{+}P < 0.01$ vs. female SCP-x$^{-/-}$ mice on the control diet.

A–D). Thus, mouse groups with little to no SCP-x (female SCP-x$^{+/+}$ and male and female SCP-x$^{-/-}$ mice) were sensitized to phytol-induced weight loss. To determine if the phytol-induced weight loss was due to reduced FTM and/or LTM, DEXA was performed at the beginning and end of the dietary experiments. DEXA scans revealed that in females, the phytol-rich diet significantly reduced FTM (3.0-fold, $P < 0.01$; Fig. 4*C*, filled bars) and less so LTM (1.3-fold, $P < 0.01$; Fig. 4*D*, filled bars), whereas in male wild-type SCP-x$^{+/+}$ mice, FTM and LTM were not significantly affected. In agreement with these results, representative DEXA images of male SCP-x$^{-/-}$ mice on the control (Fig. 4*A*) and phytol (Fig. 4B) diets indicated that phytol-fed mice appeared noticeably thinner, especially in normally fat-rich body areas, than their control diet-fed counterparts. Quantitative analysis showed that the phytol-rich diet elicited the most dramatic decrease in both FTM (7.6-fold, $P < 0.004$; Fig. 4*C*) and LTM (1.4-fold, $P < 0.004$, $n = 7$; Fig. 4*D*) in male SCP-x$^{-/-}$ mice. To a lesser extent, this effect was also observed in female SCP-x$^{-/-}$ mice (3.5- and 1.2-fold decreases in FTM and LTM, respectively, $P < 0.001$) and female SCP-x$^{+/+}$ wild-type mice (3.0- and 1.3-fold decreases in FTM and LTM, respectively, $P < 0.01$). Thus, SCP-x gene ablation sensitized male mice much more than female mice to phytol-induced FTM and less so LTM loss.

Effect of SCP-x gene ablation and dietary phytol on liver morphology and histopathology. Livers from control diet-fed male SCP-x$^{-/-}$ and female SCP-x$^{-/-}$ mice appeared grossly similar to those of control diet-fed, SCP-x$^{+/+}$ wild-type littermates. In contrast, livers from phytol-fed mice were consistently enlarged and pale with an overall mottled appearance (data not shown). In agreement with the gross assessment, histological examination of H&E-stained liver sections revealed that control diet-fed male (Fig. 7*B*) and female (Fig. 7*F*) SCP-x$^{-/-}$ mice appeared essentially normal and similar to those of control diet-fed wild-type littermates (Fig. 7, *A* and *E*, respectively). However, while the 0.5% phytol diet had no obvious effect in most male wild-type mice, there was substantial necrosis and loss of hepatocytes in all phytol-fed male (Fig. 7*D*) and female (Fig. 7*H*) SCP-x$^{-/-}$ mice in addition to

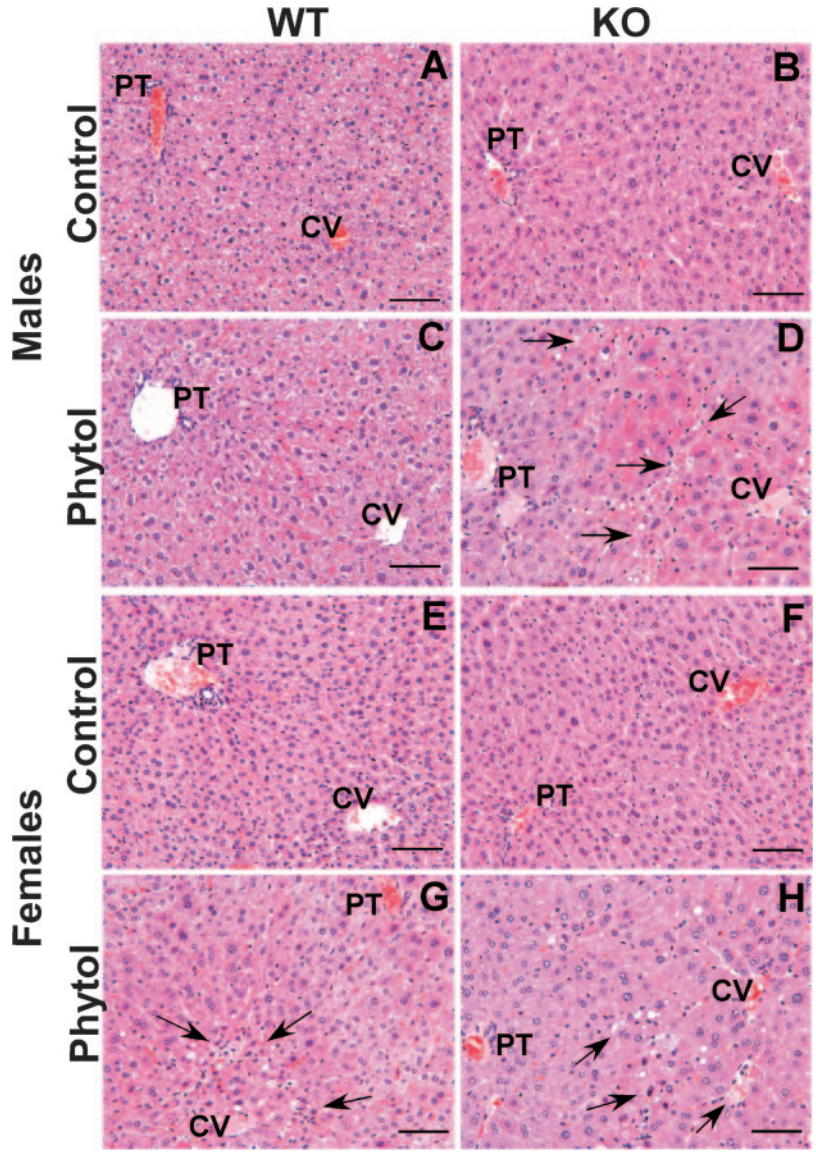

Fig. 7. Histopathology of liver tissue from male and female SCP-x$^{+/+}$ and SCP-x$^{-/-}$ mice fed a defined diet with or without 0.5% phytol. *A–H*: representative histological sections of livers stained with hematoxylin and eosin from male (*A–D*) and female (*E–H*) SCP-x$^{+/+}$ (*A*, *C*, *E*, and *G*) and SCP-x$^{-/-}$ mice (*B*, *D*, *F*, and *H*). Examples of portal triads (PT) and central veins (CV) are marked. While livers were essentially normal in control diet-fed mice and male SCP-x$^{+/+}$ mice, phytol-fed male SCP-x$^{-/-}$ mice (*D*), female SCP-x$^{+/+}$ mice (*G*), and female SCP-x$^{-/-}$ mice (*H*) exhibited necrosis and loss of some midzonal to centrilobular hepatocytes (arrows), accompanied by minor inflammation and variable hypertrophy of surviving hepatocytes. Scale bar = 75 μm.

all phytol-fed female SCP-x$^{+/+}$ wild-type mice (Fig. 7*G*). The severity of necrosis, fatty vacuolation, and inflammation were similar in all mice groups with little to no SCP-x.

Effect of SCP-x gene ablation and dietary phytol on liver lipids. To define whether SCP-x gene ablation or phytol feeding altered lipid accumulation, hepatocytes were stained with osmium tetroxide and potassium dichromate as described in MATERIALS AND METHODS to detect neutral lipids. While female liver samples exhibited significantly more lipid droplets than their male counterparts, phytol feeding resulted in substantially decreased staining in all the feeding groups examined (data not shown). SCP-x gene ablation further reduced the staining of lipid droplets in the livers of male but not female SCP-x$^{-/-}$ mice. These results were confirmed by lipid analysis. Total neutral lipids (CE + TG) in livers of female wild-type SCP-x$^{+/+}$ and SCP-x$^{-/-}$ mice had more neutral lipids than their male counterparts, consistent with the histological results. SCP-x gene ablation alone significantly decreased the neutral lipid levels in control diet-fed male as well as female mice. The phytol-rich diet significantly decreased the neutral lipid levels only in female SCP-x$^{-/-}$ mice, with a trend toward a decrease in males.

Effect of SCP-x gene ablation and dietary phytol on phytol metabolites and fatty acid class distribution. Liver homogenates from the different feeding groups were lipid extracted, transmethylated to form FAMEs, and resolved by GC/MS as described in MATERIALS AND METHODS. In livers of both female and male mice on control diets, phytanic acid was detected at similar low levels (2.2 ± 0.1 and 1.8 ± 0.2 nmol/mg protein), representing 0.8% of liver total fatty acids (Fig. 8*A*). In contrast, phytanic acid levels were increased by 1.9- and 35-fold in male and female wild-type SCP-x$^{+/+}$ mice, respectively, fed the phytol diet. SCP-x gene ablation alone decreased hepatic phytanic acid to undetectable levels in male but not female SCP-x$^{-/-}$ mice. Phytol-fed male SCP-x$^{-/-}$ mice exhibited 12-fold higher phytanic acid levels than their phytol-fed wild-type SCP-x$^{+/+}$ counterparts, whereas phytanic acid levels in phytol-fed female SCP-x$^{-/-}$ mice were not further increased. Thus, phytol-fed mice with little to no SCP-x accumulated much higher levels of phytanic acid in the liver than their male phytol-fed wild-type SCP-x$^{+/+}$ counterparts. Similar trends of phytanic acid accumulation were also observed in serum lipids (data not shown). Since accumulation of phytanic acid in the phytol-fed animals suggested a block in peroxisomal α- or β-oxidation or in thiolytic cleavage of branched-chain 3-keto-pristanoyl-CoA (a step catalyzed specifically by SCP-x), levels of other phytol metabolites were determined. Hepatic levels of pristanic acid (Fig. 8*B*), the product of peroxisomal α-oxidation of phytanoyl-CoA, were much lower than those of phytanic acid (Fig. 8*A*). In control diet-fed male and female wild-type SCP-x$^{+/+}$ mice, pristanic acid was not detected. The phytol-rich diet increased levels of hepatic pristanic acid in male and female wild-type SCP-x$^{+/+}$ mice to 6.1 ± 0.5 and 21.9 ± 0.4 nmol/mg protein, comprising 2.1% and 7%, respectively, of liver total fatty acids. SCP-x gene ablation exacerbated the effect of the phytol diet to increase pristanic acid levels to over 29- and 3.7-fold, respectively, in phytol-fed male and female SCP-x$^{-/-}$ mice. A similar trend of pristanic acid accumulation was also observed in serum lipids (data not shown). With regard to the peroxisomal β-oxidation product $\Delta^{2,3}$-pristenoic acid, this metabolite was present in control

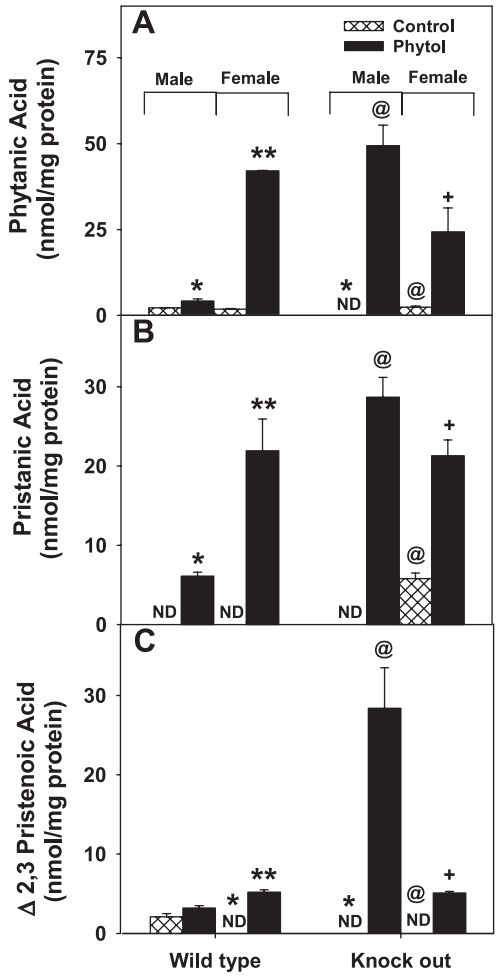

Fig. 8. Phytol metabolites in the liver. Hepatic levels of phytanic acid (*A*), pristanic acid (*B*), and $\Delta^{2,3}$-pristenoic acid (*C*) were determined in male and female SCP-x$^{+/+}$ and SCP-x$^{-/-}$ mice on control and 0.5% phytol diets as described in MATERIALS AND METHODS. Values represent means ± SE; n = 5–7 animals/group. *$P < 0.01$ vs. male WT SCP-x$^{+/+}$ mice on the control diet; **$P < 0.001$ vs. female WT SCP-x$^{+/+}$ mice on the control diet; $^{@}P < 0.001$ vs. male SCP-x$^{-/-}$ mice on the control diet; $^{+}P < 0.001$ vs. female SCP-x$^{-/-}$ mice on the control diet. ND, not detected.

diet-fed male wild-type SCP-x$^{+/+}$ mice at 2.2 ± 0.4 nmol/mg protein but was not detected in control-fed female wild-type SCP-x$^{+/+}$ mice (Fig. 8*C*). Phytol feeding increased $\Delta^{2,3}$-pristenoic acid levels in male wild-type SCP-x$^{+/+}$ mice only slightly (to 3.2 ± 0.3 nmol/mg protein) but increased levels in female wild-type SCP-x$^{+/+}$ mice significantly (i.e., 5.2 ± 0.3 nmol/mg protein, $P < 0.0001$). This trend was amplified in the SCP-x gene-ablated mice, where levels of $\Delta^{2,3}$-pristenoic acid increased from nondetectable in the control diet-fed male and female SCP-x$^{-/-}$ mice to 28.4 ± 5 and 5.1 ± 0.2 nmol/mg protein, respectively, in those fed phytol. When levels of total detectable BCFAs (i.e., phytanic acid + pristanic acid + $\Delta^{2,3}$-pristenoic acid) were described as percentages of total fatty acid, it became more clearly evident that accumulations of BCFAs were significantly higher in male SCP-x-null mice than in any other mouse group (Table 2). In male SCP-x$^{-/-}$ mice, the percentage of BCFAs increased from nondetectable (control diet) to over 30% (phytol diet). To a lesser extent, this trend was also observed in female SCP-x-null mice (2.8% vs.

Table 2. *Effect of SCP-x gene ablation on liver fatty acid class distribution*

Fatty Acid Class	Male SCP-x$^{+/+}$ Mice		Female SCP-x$^{+/+}$ Mice		Male SCP$^{-/-}$ Mice		Female SCP$^{-/-}$ Mice	
	Control diet	Phytol diet	Control diet	Phytol diet	Control diet	Phytol diet	Control diet	Phytol diet
VLCFA (C:22–26)	15±2	14±1	11±1	14±1	13±2	13±1	13±2	14±1
MCFA and LCFA (C:16–20)	85±11	86±9	89±10	86±12	87±9	87±7	87±13	86±7
BCFA	1.6±0.2	4.6±0.3*	0.7±0.1*	23±3†	ND*	30±4‡	2.8±0.4‡	20±3§

Values are means ± SE and were determined as the percent composition of the total fatty acid pool; n = 5–6 mice/group. VLCFA, very-long-chain fatty acid; MCFA, medium-chain fatty acid; LCFA, long-chain fatty acid; BCFA, branched-chain fatty acid (phytanic acid, pristanic acid, and $\Delta^{2,3}$-pristenoic acid); ND, not detected. *P<0.004 vs. male wild-type SCP-x$^{+/+}$ mice on the control diet; †P<0.001 vs. female wild-type SCP-x$^{+/+}$ mice on the control diet; ‡P<0.001 vs. male SCP-x$^{-/-}$ mice on the control diet; §P<0.01 vs. female SCP-x$^{-/-}$ mice on the control diet.

20%). Ablation of SCP-x in male mice resulted in higher accumulation of phytol metabolites compared with phytol-fed female SCP-x gene-ablated mice. In summary, increased levels of SCP-x correlated with decreased accumulation of phytol metabolites within the different mouse groups (Fig. 9). Conversely, when SCP-x levels were decreased or not present, increased accumulation of BCFAs was observed.

Since peroxisomes are the site of BCFA oxidation and also very-long-chain fatty acid (VLCFA) oxidation, a complete analysis of VLCFA (C:22–26) as well as medium- to long-chain fatty acid (C:16–20) species present in liver lipids was determined (Table 2). Upon comparison, it was shown that, regardless of diet, except for the percent BCFA, SCP-x gene ablation did not significantly affect levels of VLCFAs, medium-chain fatty acids, or long-chain fatty acids (Table 2).

Effect of SCP-x gene ablation and dietary phytol on the induction of liver peroxisomal proteins. Since phytanic acid (a phytol metabolite) is a potent peroxisome proliferator-activated receptor (PPAR)-α agonist (17), hepatic expression levels of the following PPAR-α-regulated proteins (normalized to the housekeeping gene GAPDH) were examined by Western blot analysis: peroxisomal proteins (catalase, SCP-x, SCP-2, and pThiol), intracellular cytosolic fatty acid/fatty acyl CoA binding proteins (L-FABP and ACBP), and plasma membrane transport proteins (FATP-1 and GOT). Evidence of phytol-induced peroxisome proliferation was shown by increased levels (up to 26-fold) of the peroxisomal protein marker catalase in both male and female phytol-fed mice ($P < 0.0003$; Fig. 2*G*). However, due to the already elevated levels of catalase observed in control diet-fed male (9.5-fold) and female (4.5-fold) SCP-x$^{-/-}$ mice, the phytol-rich diet elicited little or no additional increase in catalase in male and female SCP-x$^{-/-}$ mice. The phytol-rich diet increased levels of SCP-x by 5.7- and 30-fold in livers of male and female wild-type SCP-x$^{+/+}$ mice ($P < 0.0001$), respectively (Fig. 2*A*). With regard to protein levels of SCP-2, expression was significantly increased in male SCP-x$^{+/+}$ mice, with a similar trend observed with female mice on the phytol diet. In response to SCP-x gene ablation, hepatic levels of SCP-2 were increased by 2.5-and 5.4-fold in male and female SCP-x$^{-/-}$ mice, respectively ($P < 0.005$; Fig. 2*B*). However, while SCP-x gene ablation significantly increased levels of SCP-2 in control diet-fed mice, SCP-x gene ablation blunted the response to the 0.5% phytol diet such that levels of SCP-2 in phytol-fed male and female SCP-x$^{-/-}$ mice were substantially decreased by 3.6- and 2.2-fold, respectively ($P < 0.04$). Expression levels of pThiol were also determined (Fig. 5*D*). While SCP-x gene ablation alone increased levels of pThiol in control diet-fed male and female mice, the 0.5% phytol diet exacerbated this effect such that female SCP-x$^{-/-}$ mice exhibited the highest levels of pThiol of any group examined (Fig. 5*D*). Levels of L-FABP and ACBP [both regulated by PPAR-α activators such as phytanic acid and fibrates (16, 22, 48)] were regulated similarly. L-FABP expression was increased by 1.9- and 6.1-fold ($P < 0.001$) in livers of phytol-fed male and female wild-type SCP-x$^{+/+}$ mice (Fig. 2*C*). SCP-x gene ablation decreased L-FABP levels in control diet-fed male mice by 3.2-fold ($P < 0.001$), while those in female mice were increased by 2-fold ($P < 0.03$). The phytol-rich diet markedly increased L-FABP levels in liver homogenates of both male and female SCP-x$^{-/-}$ mice by 5.4- and 3-fold for males and females ($P < 0.001$). With regard to ACBP, SCP-x gene ablation decreased liver ACBP levels in control diet-fed male mice by 1.6-fold ($P < 0.001$), while those in female mice were increased by 1.6-fold ($P < 0.001$; Fig. 2*D*). The phytol diet increased ACBP levels in liver homogenates of male SCP-x$^{-/-}$ mice by 2.3-fold ($P < 0.001$) with little change in females.

With regard to the plasma membrane transport proteins FATP-1 and GOT, protein levels of FATP-1 were not significantly changed in livers of phytol-fed male or female wild-type SCP-x$^{+/+}$ mice (Fig. 2*E*). Similarly, SCP-x gene ablation

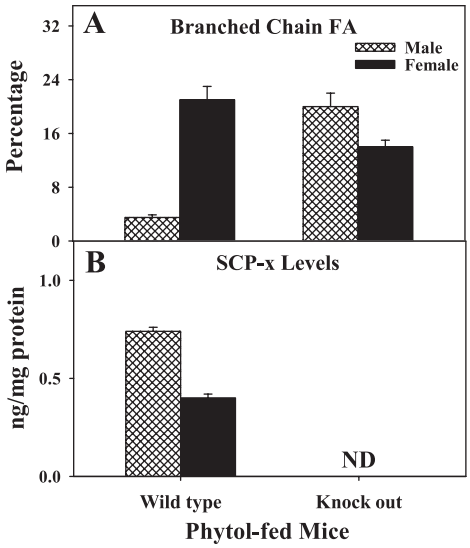

Fig. 9. Percent of branched-chain fatty acids (BCFAs) versus SCP-x levels in phytol-fed male and female SCP-x$^{+/+}$ and SCP-x$^{-/-}$ mice. Percent levels of BCFAs (*A*), including phytanic acid, pristanic acid, and $\Delta^{2,3}$-pristenoic acid, were correlated against levels of SCP-x (*B*) in phytol-fed male and female WT SCP-x$^{+/+}$ and SCP-x$^{-/-}$ mice. Values represent means ± SE; n = 5 animals/group.

did not affect liver FATP-1 levels in control diet-fed male or female mice. In contrast, the combination of phytol diet and SCP-x gene ablation resulted in a fivefold decrease in liver FATP-1 levels of male SCP-x$^{-/-}$ mice compared with their control diet-fed counterparts (Fig. 2*E*). For GOT, protein levels in liver homogenates were not significantly changed in phytol-fed male SCP-x$^{+/+}$ mice, while phytol-fed female SCP-x$^{+/+}$ mice exhibited decreased protein levels (Fig. 2*F*). In male SCP-x$^{-/-}$ mice, the expression of GOT was unaltered, and it was altered only slightly (i.e., decreased 38%) in female SCP-x$^{-/-}$ mice (Fig. 2*F*). The phytol diet markedly decreased GOT levels in liver homogenates by 2-fold in male SCP-x$^{-/-}$ mice and by 2.2-fold in female SCP-x$^{-/-}$ mice.

Effect of dietary phytol on key peroxisomal/mitochondrial enzymes. While the response with mitochondrial enzymes was less than that with peroxisomal enzymes, increased expression of several enzymes upon phytol feeding, especially in mice with little to no SCP-x, was also observed. Levels of $ACO_{pristanoyl}$ increased 1.8-, 2.5-, and 14-fold in female wild-type SCP-x$^{+/+}$, male SCP-x$^{-/-}$, and female SCP-x$^{-/-}$ mice, respectively (Fig. 5*B*). Likewise, expression levels of PBE and pThiol were significantly increased by 61- and 28-fold for PBE (Fig. 5*C*) and 2.8- and 1.6-fold for pThiol (Fig. 5*D*) in control-fed female wild-type SCP-x$^{+/+}$ and SCP-x$^{-/-}$ mice, respectively. Similarly, expression levels increased 2.5-, 2.1-, and 14-fold for mButCoADH, 1.8-, 2.7-, and 11-fold for CpT1, and 9.1-, 2.2-, and 3.3-fold for mThiol when phytol-fed female wild-type SCP-x$^{+/+}$, male SCP-x$^{-/-}$, and female SCP-x$^{-/-}$ mice, respectively, were compared with control diet-fed counterparts (Fig. 6). In summary, these data suggest that an indirect relationship exists between SCP-x levels and phytol-induced induction of several peroxisomal/mitochondrial enzymes involved in the β-oxidation of fatty acids.

DISCUSSION

Although the structure (for a review, see Ref. 37) and function (for reviews, see Refs. 19 and 40) of SCP-x and SCP-2 in BCFA and cholesterol metabolism have been investigated in vitro and in transfected cells, the origin and physiological functions of several proteins (i.e., 58-kDa SCP-x, 46-kDa thiolase, 15.2-kDa pro-SCP-2, and 13.2-kDa SCP-2) derived from the single SCP-x/SCP-2 gene have not been completely clarified. The data presented herein with SCP-x gene-ablated mice provide the following new insights. First, cleavage of 58-kDa SCP-x is not the primary source of 15.2-kDa pro-SCP-2, a protein that is rapidly and completely post-translationally cleaved to 13.2-kDa SCP-2. While it has been suggested that as much as 50% of hepatic SCP-2 is derived from the posttranslational cleavage of SCP-x (35), the present data demonstrate that SCP-x$^{-/-}$ mice exhibited increased expression of SCP-2, a result consistent with the upregulation of the second promoter region encoding the transcript for SCP-2. The basis for this response may reside in the interrelated functions of the two proteins in lipid transport and metabolism. The COOH terminus of SCP-x, containing SCP-2 entirely, confers similar cholesterol transfer activity (29), while the NH_2 terminus of SCP-x is involved in peroxisomal β-oxidation of branched-chain lipids (fatty acids and cholesterol) (14, 25, 46), ligands that SCP-2 binds with high affinity (18). Since SCP-2 also transports the respective bound ligands, targets the ligands to specific intracellular sites, and enhances the metabolism (for a review, see Ref. 19), SCP-x gene ablation and the resulting decreased ability to metabolize branched-chain ligands would necessitate a rise in SCP-2 to relieve the intracellular lipid load. Thus, differential expression of SCP2 and SCP-x could be considered as a potential mechanism through which lipid metabolism is regulated. In keeping with this, SCP-x and SCP-2 expression were differentially regulated by phytanic acid, a ligand activator of the nuclear receptor PPAR-α. While both promoter regions of the SCP-x/SCP-2 gene have peroxisomal proliferator-response elements (27, 28), expression of SCP-x was regulated independently of SCP-2, as shown by the gender-based response to dietary phytol as well as the response to SCP-x gene ablation, consistent with earlier data in diabetic rats and other models (for reviews, see Refs. 19 and 32). Since the lipid binding domain shared by SCP-2 and SCP-x exhibits a high affinity for phytanic acid (18, 48), these results are consistent with the proteins being regulated by their fatty acid substrates in a mechanism similar to many enzymes involved in peroxisomal fatty acid oxidation (i.e., ligand activation of PPAR-α).

Second, SCP-x gene ablation elicited marked accumulation of phytol metabolites in livers of phytol-fed mice. SCP-x, but not pThiol, has been shown to exhibit high activity with branched-chain 3-ketoacyl CoAs (1, 2, 46). Consistent with a metabolic block, upstream precursors of the 3-ketoacyl CoA thiolase step (i.e., phytanic acid, pristanic acid, and $\Delta^{2,3}$-pristenoic acid) accumulated in liver and serum lipids in phytol-fed SCP-x$^{-/-}$ mice. In keeping with results from in vitro studies (2, 46) with purified thiolase enzymes showing that SCP-x exhibits specificity for BCFAs, these data demonstrate, for the first time, independent of SCP-2 ablation or massive L-FABP upregulation (as shown with SCP-x/SCP-2 knockout mice), that SCP-x has a significant physiological role in BCFA oxidation in vivo. Furthermore, despite the primary location of SCP-x in peroxisomes, the site of not only BCFA oxidation but also of VLCFA oxidation, hepatic levels of VLCFA (C:22–26) were not affected by SCP-x gene ablation (Table 2), suggesting that the loss of SCP-x's role in VLCFA oxidation was compensated for by the upregulation of other thiolases still present.

Third, SCP-x gene ablation markedly sensitized male mice to the effects of dietary phytol, consistent with the gender-dependent differences observed in our earlier work (5). There is some evidence that SCP-x expression is regulated hormonally based on the fact that SCP-x expression is not sex differentiated until after puberty and maturation of the pituitary gland (36) and that a putative estrogen-response element exists within the SCP-x promoter region (34). With regard to SCP-x levels, the data showed higher accumulation of phytol metabolites upstream of the SCP-x step in all animals with little to no SCP-x. These effects were also evident from examination of the whole body phenotype, which indicated that SCP-x gene ablation sensitized not only female mice but also male knockout mice to the weight- and FTM-reducing effects of dietary phytol, despite the ingestion of similar amounts of food. The body weight and whole body fat losses in phytol-fed SCP-x$^{-/-}$ mice may be rationalized by the observed accumulation of phytol metabolites (phytanic acid and pristanic acid) binding to and activating PPAR-α to induce peroxisomal proliferation (evidenced by increased levels of catalase) and increased levels

of intracellular FATPs (e.g., SCP-2, L-FABP, and ACBP), which, in turn, resulted in decreased levels of hepatic FFA and TG levels due to increased metabolism. These findings suggest that the sexually dimorphic metabolism of branched-chain lipids may in large part be explained by differences in levels of SCP-x expression.

Finally, in response to the phytol diet, several peroxisomal enzymes responsible for oxidizing VLCFAs and BCFAs including $ACO_{pristanoyl}$, PBE, pThiol, CpT1, mButCoADH, and mThiol were highly induced in mice with little to no SCP-x. To a lesser degree, mitochondrial enzymes involved in fatty acid oxidation including CpT1, mButCoADH, and mThiol were also induced. However, despite the substantial upregulation (up to 61-fold for PBE in female SCP-$x^{+/+}$ mice) to increase fatty acid metabolism, accumulation of phytol metabolites was observed, ultimately leading to increasing signs of toxicity (i.e., reduced body weight gain and FTM along with hepatic enlargement, mottling, and necrosis). Taken together, these results further support the important physiological role for SCP-x in BCFA metabolism.

In summary, the SCP-$x^{-/-}$ mouse presents a unique model that, for the first time, allows the full examination of the role of SCP-x in fatty acid metabolism without complications arising from the loss of SCP-2 or massive upregulation of L-FABP as occurs with SCP-x/SCP-2-null mice. This becomes more important when the fact that both products of the SCP-x/SCP-2 gene promoters (i.e., SCP-x and SCP-2) as well as L-FABP are now known to be involved in peroxisomal BCFA oxidation (for reviews, see Refs. 3, 4, and 19). While SCP-x-null mice exhibited minimal changes in whole body phenotype, the present study indicates that SCP-x gene ablation markedly sensitized the response to dietary phytol. Furthermore, loss of SCP-x did not result in decreased SCP-2 expression, indicating that SCP-x was not a major source of SCP-2, as previously suggested. In conclusion, the SCP-$x^{-/-}$ mouse provides a new model to more clearly assess the role of SCP-x in the metabolism of branched-chain lipids including phytanic acid and also cholesterol (essential for the formation of bile acids) without the added complexities of concomitant SCP-2 gene ablation and L-FABP upregulation observed with SCP-x/SCP-2 double-knockout mice.

ACKNOWLEDGMENTS

The technical assistance of Amy Boedeker, Kerstin Landrock, and Bhuvanendran Shivaprasad was much appreciated.

GRANTS

This work was supported in part by National Institutes of Health Grants DK-41402 (to F. Schroeder and A. B. Kier), GM-31651 (to F. Schroeder and A. B. Kier), and P30-ES-09106 (to B. P. Atshaves and A. B. Kier).

REFERENCES

1. **Antonenkov VD, Van Veldhoven PP, Mannaerts GP.** Isolation and subunit composition of native sterol carrier protein-2/3-oxoacyl-coenzyme A thiolase from normal rat liver peroxisomes. *Protein Expr Purif* 18: 249–256, 2000.
2. **Antonenkov VD, Van Veldhoven PP, Waelkens E, Mannaerts GP.** Substrate specificities of 3-oxoacyl-CoA thiolase A and sterol carrier protein 2/3-oxoacyl-CoA thiolase purified from normal rat liver peroxisomes. *J Biol Chem* 272: 26023–26031, 1997.
3. **Atshaves BP, McIntosh AL, Lyuksyutova OI, Zipfel WR, Webb WW, Schroeder F.** Liver fatty acid binding protein gene ablation inhibits branched-chain fatty acid metabolism in cultured primary hepatocytes. *J Biol Chem* 279: 30954–30965, 2004.
4. **Atshaves BP, McIntosh AL, Payne HR, Mackie J, Kier AB, Schroeder F.** Effect of branched-chain fatty acid on lipid dynamics in mice lacking liver fatty acid binding protein gene. *Am J Physiol Cell Physiol* 288: C543–C558, 2005.
5. **Atshaves BP, Payne HR, McIntosh AL, Tichy SE, Russell D, Kier AB, Schroeder F.** Sexually dimorphic metabolism of branched chain lipids in C57BL/6J mice. *J Lipid Res* 45: 812–830, 2004.
6. **Atshaves BP, Petrescu A, Starodub O, Roths J, Kier AB, Schroeder F.** Expression and intracellular processing of the 58 kDa sterol carrier protein 2/3-oxoacyl-CoA thiolase in transfected mouse L-cell fibroblasts. *J Lipid Res* 40: 610–622, 1999.
7. **Atshaves BP, Storey SM, Petrescu AD, Greenberg CC, Lyuksyutova OI, Smith R, Schroeder F.** Expression of fatty acid binding proteins inhibits lipid accumulation and alters toxicity in L-cell fibroblasts. *Am J Physiol Cell Physiol* 283: C688–C703, 2002.
8. **Atshaves BP, Storey SM, Schroeder F.** Sterol carrier protein-2/sterol carrier protein-x expression differentially alters fatty acid metabolism in L-cell fibroblasts. *J Lipid Res* 44: 1751–1762, 2003.
9. **Berk PD, Wada H, Horio Y, Potter BJ, Sorrentino D, Zhou SL, Isola LM, Stump D, Kiang CL, Thung S.** Plasma membrane fatty acid binding protein and mitochondrial glutamic-oxaloacetic transaminase of rat liver are related. *Proc Natl Acad Sci USA* 87: 3484–3488, 1990.
10. **Bradbury MW.** Lipid metabolism and liver inflammation. I. Hepatic fatty acid uptake: possible role in steatosis. *Am J Physiol Gastrointest Liver Physiol* 290: G194–G198, 2006.
11. **Bradbury MW, Berk PD.** Cellular uptake of long chain free fatty acids: the structure and function of plasma membrane fatty acid binding protein. *Adv Mol Cell Biol* 33: 47–80, 2004.
12. **Bradford M.** A rapid and sensitive method for the quantitation of microgram quantities of protein utilizing the principle of protein dye binding. *Anal Biochem* 72: 248–254, 1976.
13. **Bradley A.** Production and analysis of chimeric mice. In: *Teratocarcinomas and Embryonic Stem Cells: a Practical Approach*, edited by Robertson EJ. Oxford: Oxford/IRL, 1987.
14. **Bun-ya M, Maebuchi M, Kamiryo T, Kurosawa T, Sato M, Tohma M, Jiang LL, Hashimoto T.** Thiolase involved in bile acid formation. *J Biochem* 123: 347–352, 1998.
15. **Clarke DC, Miskovic D, Han XX, Calles-Escandon J, Glatz JF, Luiken JJFP, Heikkila JJ, Bonen A.** Overexpression of membrane associated fatty acid binding protein (FABPpm) in vivo increases fatty acid sarcolemmal transport and metabolism. *Physiol Genomics* 17: 31–37, 2004.
16. **Desvergne B, Wahli W.** Peroxisome proliferator activated receptors: nuclear control of metabolism. *Endocr Rev* 20: 649–688, 1999.
17. **Ellinghaus P, Wolfrum C, Assmann G, Spener F, Seedorf U.** Phytanic acid activates the peroxisome proliferator-activated receptor alpha (PPARalpha) in sterol carrier protein-2-/sterol carrier protein x-deficient mice. *J Biol Chem* 274: 2766–2772, 1999.
18. **Frolov A, Miller K, Billheimer JT, Cho TC, Schroeder F.** Lipid specificity and location of the sterol carrier protein-2 fatty acid binding site: a fluorescence displacement and energy transfer study. *Lipids* 32: 1201–1209, 1997.
19. **Gallegos AM, Atshaves BP, Storey SM, Starodub O, Petrescu AD, Huang H, McIntosh A, Martin G, Chao H, Kier AB, Schroeder F.** Gene structure, intracellular localization, and functional roles of sterol carrier protein-2. *Prog Lipid Res* 40: 498–563, 2001.
20. **Hall PF, Gormley BM, Jarvis LR, Smith RD.** A staining method for the detection and measurement of fat droplets in hepatic tissue. *Pathology* 12: 605–608, 1980.
21. **Hara A, Radin NS.** Lipid extraction of tissues with a low toxicity solvent. *Anal Biochem* 90: 420–426, 1978.
22. **Hellendie T, Grontved L, Jensen SS, Kiilerich P, Rietveld L, Albrektsen T, Boysen MS, Nohr J, Larsen LK, Fleckner J, Stunnenberg HG, Kristiansen K, Mandrup S.** The gene encoding the acyl CoA binding protein is activated by peroxisome proliferator activated receptor gamma through an intronic response element functionally conserved between humans and rodents. *J Biol Chem* 277: 26821–26830, 2002.
23. **Hooper M, Hardy KK, Handyside A, Hunter S, Monk M.** HPRT deficient (Lesch-Nyham) mouse embryos derived from germline colonisation by cultured cells. *Nature* 326: 292–295, 1987.

24. **Huang H, Ball JA, Billheimer JT, Schroeder F.** The sterol carrier protein-2 amino terminus: a membrane interaction domain. *Biochemistry* 38: 13231–13243, 1999.
25. **Jakobs BS, Wanders RJA.** Conclusive evidence that very-long-chain fatty acids are oxidized exclusively in peroxisomes in human skin fibroblasts. *Biochem Biophys Res Commun* 178: 842–847, 1997.
26. **Livak KJ, Schmittgen TD.** Analysis of relative gene expression data using real-time quantitative PCR and the $2^{-\Delta\Delta CT}$ method. *Methods* 25: 402–408, 2001.
27. **Lopez D, Irby RB, McLean MP.** Peroxisome proliferator-actiated receptor alpha induces rat sterol carrier portein x promoter activity through two peroxisome proliferator response elements. *Mol Cell Endocrinol* 205: 169–184, 2003.
28. **Lopez D, Shea-Eaton W, McLean MP.** Characterization of a steroidogenic factor-1 binding site found in promoter of sterol carrier protein-2 gene. *Endocrine* 14: 253–261, 2001.
29. **Manfra DJ, Baum CL, Reschley E, Lundell D, Zavodny P, Dalie B.** Expression and purification of two recombinant sterol-carrier proteins: SCPX and SCP2. *Protein Expr Purif* 6: 196–205, 1995.
30. **Maniatis T, Fritsch EF, Sambrook J.** *Molecular Cloning. A Laboratory Manual.* Cold Spring Harbor, NY: Cold Spring Harbor Laboratory Press, 1989.
31. **Marzo A, Ghirardi P, Sardini D, Meroni G.** Simplified measurement of monoglycerides, diglycerides, triglycerides, and free fatty acids in biological samples. *Clin Chem* 17: 145–147, 1971.
32. **McLean MP, Warden KJ, Sandoff TW, Irby RB, Hales DB.** Altered ovarian sterol carrier protein-2 expression in pregnant streptozotocin treated diabetic rat. *Biol Reprod* 55: 38–46, 1996.
33. **Monnig G, Wiekowski J, Kirchhof P, Stypmann J, Plenz G, Fabritz L, Bruns HJ, Eckardt L, Assmann G, Haverkamp W, Breithardt G, Seedorf U.** Phytanic acid accumulation is associated with conduction delay and sudden cardiac death in sterol carrier protein-2/sterol carrier protein-x deficient mice. *J Cardiovasc Electrophysiol* 15: 1310–1316, 2004.
34. **Ohba T, Holt JA, Billheimer JT, Strauss JFI.** Human sterol carrier protein x/sterol carrier protein 2 gene has two promoters. *Biochemistry* 34: 10660–10668, 1995.
35. **Ossendorp BC, Voorhout WF, Van Amerongen A, Brunink F, Batenburg JJ, Wirtz KWA.** Tissue-specific distribution of a peroxisomal 46-kDa protein related to the 58-kDa protein (sterol carrier protein X; sterol carrier protein 2/3-oxoacyl-CoA thiolase). *Arch Biochem Biophys* 334: 251–260, 1996.
36. **Roff CF, Pastuszyn A, Strauss JFI, Billheimer JT, Vanier MT, Brady RO, Scallen TJ, Pentchev PG.** Deficiencies in sex-regulated expression and levels of two hepatic sterol carrier proteins in a murine model of Niemann-Pick type C disease. *J Biol Chem* 267: 15902–15908, 1992.
37. **Schroeder F, Frolov A, Starodub O, Russell W, Atshaves BP, Petrescu AD, Huang H, Gallegos A, McIntosh A, Tahotna D, Russell D, Billheimer JT, Baum CL, Kier AB.** Pro-sterol carrier protein-2: role of the N-terminal presequence in structure, function, and peroxisomal targeting. *J Biol Chem* 275: 25547–25555, 2000.
38. **Seedorf U, Assmann G.** The role of PPARalpha in obesity. *Nutr Metab Cardiovasc Dis* 11: 189–194, 2001.
39. **Seedorf U, Brysch P, Engel T, Schrage K, Assmann G.** Sterol carrier protein X is peroxisomal 3-oxoacyl coenzyme A thiolase with intrinsic sterol carrier and lipid transfer activity. *J Biol Chem* 269: 21277–21283, 1994.
40. **Seedorf U, Ellinghaus P, Nofer JR.** Sterol carrier protein-2. *Biochim Biophys Acta* 1486: 45–54, 2000.
41. **Seedorf U, Raabe M, Ellinghaus P, Kannenberg F, Fobker M, Engel T, Denis S, Wouters F, Wirtz KWA, Wanders RJA, Maeda N, Assmann G.** Defective peroxisomal catabolism of branched fatty acyl coenzyme A in mice lacking the sterol carrier protein-2/sterol carrier protein-x gene function. *Genes Dev* 12: 1189–1201, 1998.
42. **Spady DK, Woollett LA, Dietschy JM.** Regulation of plasma LDL-cholesterol levels by dietary cholesterol and fatty acids. *Annu Rev Nutr* 13: 355–381, 1993.
43. **Steinberg D.** Refsums disease. In: *The Metabolic and Molecular Basis of Inherited Disease*, edited by Scriver CR, Beaudet AL, Sly WS, Vallee D. New York: McGraw-Hill, 1995, p. 2351–2370.
44. **Van Veldhoven PP, Vanhove GF, Asselberghs S, Eyssen HJ, Mannaerts GP.** Substrate specificities of rat liver peroxisomal acyl-CoA oxidases: palmitoyl-CoA oxidase (inducible acyl CoA oxidase), pristanoyl-CoA oxidase (noninducible acyl CoA oxidase), and trihydroxycoprostanoyl-CoA oxidase. *J Biol Chem* 267: 20065–20074, 1992.
45. **Verhoeven NM, Wanders RJA, Poll-The BT, Saudubray JM, Jakobs C.** The metabolism of phytanic acid and pristanic acid in man: a review. *J Inherit Metab Dis* 21: 697–728, 1998.
46. **Wanders RJ, Denis S, van Berkel E, Wouters F, Wirtz KWA, Seedorf U.** Identification of the newly discovered 58 kDa peroxisomal thiolase SCP-x as the main thiolase involved in both pristanic acid and trihydroxycholestanoic acid oxidation: implications for peroxisomal beta-oxidation disorders. *J Inherit Metab Dis* 21: 302–305, 1998.
47. **Wanders RJ, van Roermund CW.** Studies on phytanic acid alpha-oxidation in rat liver and cultured human skin fibroblasts. *Biochim Biophys Acta* 1167: 345–350, 1993.
48. **Wolfrum C, Ellinghaus P, Fobker M, Seedorf U, Assmann G, Borchers T, Spener F.** Phytanic acid is ligand and transcriptional activator of murine liver fatty acid binding protein. *J Lipid Res* 40: 708–714, 1999.
49. **Wouters F, Bastiaens PI, Wirtz KW, Jovin TM.** FRET microscopy demonstrates molecular association of non-specific lipid transfer protein (nsL-TP) with fatty acid oxidation enzymes. *EMBO J* 17: 7179–7189, 1998.